# BRINZOLAMIDE-LOADED ETHO-LECIPLEX FOR EFFECTIVE OCULAR MANAGEMENT OF GLAUCOMA: D-OPTIMAL DESIGN OPTIMIZATION AND *IN VIVO* EVALUATION

## SARA NAGEEB EL-HELALY[1], HAYDER A. HAMMOODI[2*], MINA I. TADROS[1,3], NERMEEN A. ELKASABGY[1]

[1]Department of Pharmaceutics and Industrial Pharmacy, Faculty of Pharmacy, Cairo University, Kasr El-Aini Street-11562 Cairo, Egypt.
[2]Department of Pharmacy, Mazaya University College, Thi-Qar, Iraq. [3]Department of Pharmaceutics, Faculty of Pharmacy and Drug Technology, Egyptian Chinese University, Cairo, Egypt
*Corresponding author: Hayder A. Hammoodi; *Email: dr212hay@gmail.com

## ABSTRACT

**Objective:** Brinzolamide (BRZ) is an active carbonic anhydrase inhibitor adopted for glaucoma management. The limited aqueous solubility of the drug restricts its potential for ocular administration. Therefore, the aim of this investigation was to design a nanocarrier system called Etho-Leciplex (Etho-LPs) for the delivery of BRZ.

**Methods:** Etho-LPs were fabricated by a simple one-step technique and then optimized by D-optimal design employing Phospholipon®90G (PC): surfactant ratio and surfactant type (Cetyl Trimethyl Ammonium Bomide (CTAB) and Searylamine; SA) as independent variables, whereas the dependent variables were Entrapment Efficiency (EE%), Particle Size (PS), Polydispersity Index (PDI), and Zeta Potential (ZP). Design Expert® statistically suggested the optimum Etho-LP, which consisted of PC: Surface Active Agent (SAA) molar ratio ($X_1$) of 1:1.27 and mixture of CTAB and SA ($X_2$) in 1:1 molar ratio.

**Results:** The optimum Etho-LPs particles had spherical morphology, and EE% of 91.12±0.2 %, PS of 76.21±1.21 nm, PDI of 0.421±0.001 and ZP of 35.88 ±0.10 mV. The *in vitro* release study results demonstrated that BRZ is rapidly liberated from the optimum Etho-LPs compared to BRZ-suspension. Further, the optimum Etho-LP showed good mucoadhesive properties besides potential safety on rabbits' eyes tissues. The optimum Etho-LP was found to enhance the ocular bioavailability of the drug in rabbits' eyes relative to the BRZ suspension. In addition, histopathological assessment indicated the safety of BRZ-loaded Etho-LPs.

**Conclusion:** Overall, the obtained outcomes indicated the effectiveness of employing Etho-LPs for the treatment of glaucoma.

**Keywords:** Brinzolamide, Etho-leciplex, Glaucoma, D-optimal design, *In vivo* study

## INTRODUCTION

Glaucoma is characterized as an optic neuropathy that demonstrates a gradual progression, evident through the excavation of the optic nerve head and a decrease in visual sensitivity. This condition typically originates in the mid-peripheral visual field [1]. Elevated Intraocular Pressure (IOP) is a significant risk factor associated with the progressive deterioration of the optic nerve and consequent loss of visual field in individuals diagnosed with glaucoma or ocular hypertension [2]. Glaucoma may be either open-angle or closed-angle. Open-angle glaucoma is the prevailing manifestation of glaucoma, characterized by a gradual onset, whereas closed-angle glaucoma happens abruptly [3]. The primary focus of glaucoma management is the reduction of IOP, which is widely recognized as the principal therapeutic approach [4]. The pharmacological management of glaucoma encompasses the administration of medications belonging to diverse categories, including prostaglandin analogs [5], beta-blockers [6], carbonic anhydrase inhibitors [7], adrenergic agonists [8], miotics, and hyperosmotic agents [9]. According to Yadav *et al.*, several medication categories are known to either enhance aqueous humor outflow or decrease its production inside the ocular system [10].

Brinzolamide (BRZ) is a topically active carbonic anhydrase inhibitor obtained from a family of heterocyclic sulfonamides utilized to decrease and manage high IOP [11, 12]. Its poor aqueous solubility (0.713 mg/ml in aqueous humor) limited its clinical use [13]. The commercial formulation of BRZ named Azopt® is an aqueous suspension comprised of 1% (w/v) BRZ. Unfortunately, this preparation is coupled with shortcomings, such as blurred vision, pain, dry eye, eye discharge, blepharitis, and taste perversion. It has short contact time, poor infiltration, pre-corneal loss and poor bioavailability [14]. Hence, trials to overcome these limitations should be introduced.

Ocular drug delivery through using lipid nanocarriers has been the target of several research works [15]. Lipid nanocarriers include mixed micelles [16], cubosomes [17], proniosomes [18], and leciplex

[19]. Biocompatibility and mucoadhesive properties of nanocarriers augment their contact with the ocular mucosa, which might extend the corneal contact time of the entrapped drug, augmenting its ocular bioavailability, and decreasing both local and systemic shortcomings [20, 21]. In addition, nanoparticles possess the potential to cross the blood-retinal barriers, resulting in augmented ocular permeability and increased bioavailability [22-24]. In general, nanocarriers could be intended to treat the most vital ocular illnesses, such as ocular inflammation or infection, glaucoma, or diseases impacting the shape from of the posterior eye [25].

Leciplex is a positively charged lipid nanocarrier intended for the improvement of conveyance of different bioactives [26, 27]. It is comprised of a lipid (phospholipid), cationic surface-active agent and Transcutol® as a biocompatible solvent [28]. It has a privilege over the conventional lipid nanocarriers related to its simplicity of production in a single step [29]. It has been utilized for skin conveyance of idebenone and azelaic acid [30], oral administration of quercetin [31] and ocular delivery of carvedilol [19]. Previous investigations assessed the use of ethanol (as a solvent in addition to a penetration enhancer) in the leciplexformulation instead of Transcutol® and the preparation of a developed nanocarrier called Etho-Leciplex (Etho-LPs) for cutaneous delivery of minoxidil [32].

To the authors' knowledge, there is no scientific investigation evaluated the impact of Etho-LPs to enhance the deposition of BRZ for managing glaucoma in ocular tissues. Hence, this study aimed to evaluate Etho-LPs' ability to improve BRZ ocular retention and investigate its safety. To attain this, several variables affecting particles responses were inspected employing D-optimal design using Design Expert® software to elect the optimum Etho-LPs. The prepared Etho-LPs were assessed for their entrapment efficiency, particle size, polydispersity index and zeta potential. The optimum Etho-LPs were evaluated for its *in vitro* drug release morphological shape besides the effect of storage. Finally, *in vivo* studies of the

optimum Etho-LPs as well as histopathological studies, were accomplished in male Albino rabbits.

## MATERIALS AND METHODS

### Materials

Brinzolamide (BRZ) was acquired from Dalian Meilun Biology Technology (Dalian, China). Phospholipon® 90 G (PC; from soybean (90%) was a gift from lipoid GmbH, Ludwigshafen, Germany). Cetyl Trimethyl Ammonium Bromide (CTAB), Stearyl Amine (SA), mucin from porcine stomach type II, were bought from Sigma-Aldrich Co. (St. louis, MO, USA). Acetonitrile and ethanol were acquired from Merck (Darmstadt, Germany). All other compounds utilized in the experiment were of analytical grade and were employed in their original form.

### Preparation of BRZ-loaded Etho-LPs

Etho-LPs were prepared applying a simple one-step technique. In brief, PC and the used surfactant (SAA) were mixed in glass vials followed by the addition of 50 mg BRZ. The mixture was dissolved in ethanol (0.5 ml). Subsequently, 4.5 ml of bi-distilled water were added dropwise to the mixture at the same temperature. The process involved continuous mixing using a digital hotplate magnetic stirrer (LX653DMS, LabDex, London, UK) operating at 1200 rpm for 30 min at 70 °C [33]. The Etho-LPs dispersion was incubated at 4 °C overnight to allow for the development of fully formed particles.

### Optimization of BRZ-loaded Etho-LPs by D-optimal design

The study employed a D-optimal design methodology to investigate the effects of various parameters on the formation of Etho-LPs using the Design Expert®software (Stat-Ease, Minneapolis, MN, USA). The formation of Etho-LPs involved the examination of two independent variables: $X_1$, which represents the molar ratio of PC to SAA, and $X_2$, which signifies the type of SAA used. The dependent variables chosen for this study were Entrapment Efficiency (EE%; $Y_1$), Particle Size (PS; $Y_2$), Polydispersity Index (PDI; $Y_3$), and Zeta Potential (ZP; $Y_4$). The design is elucidated in table 1, while the composition of the created formulations is compiled in table 2.

**Table 1: D-optimal design for optimization of brinzolamide-loaded Etho-LPs**

| Factors (independent variables) | Levels | | |
|---|---|---|---|
| | Low | Medium | High |
| $X_1$: PC: SAA molar ratio | 1:1 | 1:2 | 1:3 |
| $X_2$: Type of SAA | CTAB | SA | CTAB+SA* |
| Responses (dependent variables) | Desirability Constraints | | |
| $Y_1$: EE% | Maximize | | |
| $Y_2$: PS (nm) | Minimize | | |
| $Y_3$: PPI | Minimize | | |
| $Y_4$: ZP (mV) | Maximize | | |

*Ratio of SAA mixture; CTAB: SA = 1:1 molar ratio. Abbreviations: CTAB; Cetyl Trimethyl Ammonium Bromide, SA; Stearyl Amine, EE%; Entrapment Efficiency Percent, PS; Particle Size, PDI; Polydispersity Index, PC; Phospholipid, ZP; Zeta Potential; SAA; Surface Active Agent, and Etho-lPs; Etholeciplex.

**Table 2: Experimental runs, independent variables, and measured response of the d-optimal experimental design of brinzolamide-loaded Etho-LPs**

| Formulation code | PC: SAA ratio | Type of SAA* | EE (%) | PS (nm) | PDI | ZP (mV) |
|---|---|---|---|---|---|---|
| F1 | 1:1 | CTAB+SA | 90.59±0.05 | 75.20±2.47 | 0.450±0.120 | 31.75±0.02 |
| F2 | 1:2 | CTAB | 88.44±0.11 | 67.20±1.78 | 0.318±0.110 | 38.49±0.04 |
| F3 | 1:3 | CTAB+SA | 56.91±0.20 | 79.85±5.00 | 0.523±0.100 | 41.34±0.13 |
| F4 | 1:2.5 | SA | 77.02±0.78 | 92.00±6.00 | 0.481±0.001 | 37.00±1.00 |
| F5 | 1:1 | SA | 86.86±0.12 | 127.50±4.50 | 0.481±0.000 | 21.00±2.00 |
| F6 | 1:1 | CTAB+SA | 90.80±0.12 | 74.02±1.95 | 0.440±0.200 | 31.03±0.78 |
| F7 | 1:1 | CTAB | 92.87±0.20 | 111.40±2.60 | 0.350±0.210 | 35.50±0.52 |
| F8 | 1:3 | CTAB | 67.65±0.23 | 25.80±10.50 | 0.567±0.010 | 42.23±1.23 |
| F9 | 1:3 | SA | 53.95±0.12 | 83.00±4.00 | 0.327±0.002 | 51.37±1.56 |
| F10 | 1:3 | CTAB+SA | 57.29±0.91 | 80.42±2.67 | 0.521±0.030 | 40.53±1.34 |
| F11 | 1:2 | SA | 79.62±0.32 | 125.80±10.50 | 0.413±0.100 | 38.02±1.20 |
| F12 | 1:1 | SA | 86.01±0.01 | 124.00±20.00 | 0.480±0.008 | 22.00±.090 |
| F13 | 1:1.5 | CTAB | 90.28±0.82 | 81.20±1.20 | 0.469±0.010 | 37.18±0.60 |

*Ratio of SAA mixture; CTAB: SA = 1:1 molar ratio, Abbreviations: CTAB; Cetyltrimethylammonium Bromide, SA; stearyl amine, EE%; Entrapment Efficiency Percent, PS; Particle Size, PDI; Polydispersity Index, PC; Phospholipid, ZP; Zeta Potential; SAA; Surface Active Agent, and Etho-lPs; Etholeciplex. The data is given in mean±SD.

### Characterization of BRZ-loaded Etho-LPs

### Determination of entrapment efficiency %

One milliliter volume of Etho-LPs was subjected to centrifugation at a speed of 12,000 rpm for 1 h at 4 °C using a cooling centrifuges (Sigma 3K 30, Germany). The supernatant was transferred to a volumetric flask and appropriately diluted with bi-distilled (10 ml). Subsequently, the concentration of BRZ was determined at a wavelength of maximum absorption ($\lambda_{max}$) of 254 nm using a UV-VIS spectrophotometer (Shimadzu UV1650, Japan). The EE% was calculated using the subsequent equation [31, 33].

$$EE\% = \left(\frac{\text{Total amount of BRZ} - \text{Unentrapped BRZ}}{\text{Total amount of BRZ}}\right) \times 100 \quad ..... \text{(Eq. 1)}$$

### Determination of particle size (PS), Polydispersity index (PDI), and zeta potential (ZP)

PS, PDI, and ZP of the formed Etho-LPs were assessed using the Zetasizer Nano ZS (Malvern Instruments ltd., Malvern, UK). The assessments were conducted following appropriate dilution. The evaluation of ZP was conducted through the observation of the electrophoretic mobility of the particles inside an electric field [35].

### Selecting the optimum BRZ-Etho-LPs

The optimal Etho-LPs was opted by employing Design Expert® software version 7 (Stat Ease, Inc., Minneapolis, MN, USA), which facilitated a comprehensive analysis of the replies [36]. The optimal Etho-LPs were determined by selecting the formulation with the

lowest PS and PDI, as well as the highest EE% and ZP. To evaluate the efficacy of the model, the formulation was developed, thoroughly examined, and then compared to the predicted answers [37].

### *In vitro* release study

The study was conducted using the dialysis bag technique. The BRZ suspension and optimal Etho-LPs, equivalent to 10 mg BRZ, were introduced into dialysis bags that had been pre-soaked in distilled water for 12 h. Subsequently, the filled bags were securely sealed and placed into stoppered bottles containing 80 ml of phosphate-buffered saline (PBS; pH of 7.4). The bottles were located in a shaking water bath (Unimax, IKA, Staufen, Germany) and operated at 100 strokes per minute at a temperature of 32±0.5 ℃. At certain intervals; 0.25, 0.5, 0.75, 1, 1.5, 2, 3, 4, 6, 8, 12, and 24 h), 1 ml of the release medium was withdrawn and compensated with equal volume of the fresh release medium. The samples were assessed utilizing a UV spectrophotometer at a wavelength of maximum absorption ($\lambda_{max}$) of 254 nm.

The release data; Q2 and Q24, which represents the percentage of medication released after 24 h, was utilized as a means of comparison. The statistical significance of the obtained data was assessed applying a student t-test conducted using SPSS® software version 22.0 (SPSS Inc., Chicago, USA).

### pH assessment

The pH of the optimum Etho-LPs was evaluated, by a calibrated pH meter (Hanna, type 211, Romania).

### Differential scanning calorimetry (DSC)

The thermal evaluation of BRZ and the lyophilized-optimum Etho-LPs were performed by DSC (Shimadzu Corp., Japan) standardized with indium. Samples (5 mg) were positioned in standard aluminum pan and heated in a range of 10-250 °C at a rate of 5 °C/min below nitrogen stream.

### Transmission Electron Microscope (TEM)

The external morphology of the optimum Etho-LPs was investigated by means of a TEM (JEM-1230, Tokyo, Japan) operated at 80 kV. Diluted Etho-LPs were added on carbon carbon-coated grid and stained with a 1% phosphotungstic acid then visualized [38].

### Mucoadhesion test

To assess the ability of the examined formulation to adhere to the ocular mucous membrane, a mucoadhesion test was performed. In brief, the optimal Etho-LPs was mixed with a 1% v/v mucin solution in a ratio of 1:1 (v/v), then vortexed for 2 min [39]. The ZP of the prepared combinations was determined using the ZetaSizer Nano ZS instrument.

### Effect of short-term storage

The effect of storage of the optimum Etho-LPs under refrigeration (4±0.5 ℃) for 3 mo was examined. The preserved samples were visually examined to identify any aggregates [40] and also their EE%, PS, PDI, and ZP were compared with those of the fresh samples. Statistical significance was determined through the application of a paired Student's t-test using SPSS® software version 22.0 (SPSS Inc., Chicago, USA). A non-significant difference is considered at p-value greater than 0.05.

### *In vivo* study

### Ethical approval statement

The study protocol was reviewed and approved by the Research Ethical Committee, Faculty of Pharmacy, Cairo University (PI3348). The study was conducted on male Albino rabbits as they have large eyes as well as being more vulnerable to any irritating materials compared to human's eyes [41]. The utilization and management of animals in all research endeavors adhered to the Guide for the Care and Use of laboratory Animals of the National Institutes of Health (NIH publication No.85–23, 1996) and ARRIVE guidelines 2.0. The animals were housed in cages at ambient temperature. They were subjected to a light-dark cycle of 12 h each. They were supplied by a standard meal and unrestricted access to water.

### Study design and dosing

The investigated samples were the optimum BRZ-loaded Etho-LPs besides the drug suspension (10 mg/ml). A total of 16 male Albino rabbits (2.0-2.5 Kg) were enrolled in the *in vivo* studies; pharmacokinetic and histopathological studies. The animals were allocated into two equal groups (n=8). A non-blind, parallel, single-dose design was adopted where a drop of each investigated sample (50 μl) was applied into the conjunctival sac of the rabbit's eye.

### Tear film sampling

Tear samples were gathered by carefully (to avoid any irritation to eyelids) placing 3 sterile filter paper discs (6 mm in diameter) beneath the lower eyelid of the rabbit's eye for a period of 30 s. The sampling points were at 0.5, 1, 2, 4, 6, 9 and 24 h. Following, the collected discs at each time point were stored in Eppendorf tubes at −20 ℃filled with 1 ml of acetonitrile-water (70:30 %v/v) pending analysis.

### Assay method

The frozen samples were thawed at room temperature. The analysis of BRZ in plasma samples was done utilizing a modified liquid chromatography-mass spectrometry (LC/MS/MS) method characterized by enhanced sensitivity, accuracy, and selectivity [42]. A volume of 0.5 ml of the samples was transferred into the autosampler vials of the LC/MS/MS system. The experimental setup utilized a Shimadzu Prominence series lC system (Shimadzu Scientific Instruments, Columbia, MD). The lC system consisted of a degasser (DGU-20A3) and a solvent delivery unit (LC-20AB), in addition to an autosampler (SIL-20 AC). Samples of 20 μL were injected into a Sunfire C18 column (50*4.6 mm) with a stationary phase composed of a 5-micron adsorbent provided by (Phenomenex Inc. Torrance, CA). The guard column utilized in this study was a Phenomenex C18 column (5*4 mm). The column contained particles with a size of 5 microns. The mobile phase used in this study was an isocratic mixture of 70% acetonitrile, 30% water, and 0.1% formic acid. It was supplied at a flow rate of 0.5 ml/min into the electrospray ionization chamber of the mass spectrometer. Quantitative analysis was conducted using MS/MS detection in the negative ion mode. The instrument utilized for this purpose was an MDS Sciex (Foster City, CA) API-3200 mass spectrometer, which was equipped with a turbo ion spray interface operating at a temperature of 450℃ The ion spray voltage was adjusted to a value of 4500 V. The standard parameters, namely curtain gas, nebulizer gas, collision gas, and auxiliary gas, were established at 10 psi, 20 psi, 6 psi, and 40 psi, correspondingly. The values of the compound parameters, namely the delustering potential, collision energy, entry potential, and collision exit potential, were measured to be 71, 17, 10.5, and 26 V, respectively. The ions were detected using multiple reactions monitoring mode, specifically monitoring the transition of the precursor ion with m/z 384 to the production with m/z 384. The quadrupoles Q1 and Q3 were adjusted to achieve a resolution of one unit. The data analysis was conducted using Analyst Software Version 1.6 (AB Sciex Pte. ltd., Woodlands, Singapore).

### Pharmacokinetic parameters and statistical analysis

The pharmacokinetic parameters of BRZ in the tear film were determined using Kinetica® software (Thermo Fisher Scientific Inc. Waltham, MA). The maximum concentration of BRZ in tear film ($C_{max}$) and the time taken to attain this maximum concentration ($T_{max}$), as well as the area under the concentration-time curve until the last measurable point ($AUC_{0-24}$), were computed. The pharmacokinetic parameters were statistically analyzed applying a One-Way Analysis of Variance (ANOVA).

### Histopathological study

To assess the safety of the developed formulation, a histopathological test was conducted. In brief, three rabbits (2.0-2.5 Kg) were used, where each received 3 daily doses of the selected Etho-LPs for a period of 7 d in the right eye, while the left eye was kept as a control. After one week, the rabbits were humanly decapitated after administering ketamine (600 mg, intravenously) [43]. Following, the whole eyeballs were removed and cleaned with saline prior to fixation in formalin saline solution for one day (10% v/v). The bodies of the rabbits were frozen and incinerated. Specimens were dehydrated using ethyl alcohol then fixed in paraffin blocks at 56 °C for 24 h. Microtome (Leica SM2400, Cambridge, UK) was used to prepare thin slices (4 μm), which were

deparaffinized and pigmented with hematoxylin and eosin. Finally, the samples were inspected by means of a light microscope (Leica, Cambridge, UK) [44].

## RESULTS AND DISCUSSION

### D-optimal design optimization

In order to determine the ranges of the independent variables, preliminary experiments were carried out (data not shown here). The independent variables examined for the formation of Etho-LPs included $X_1$, which represents the molar ratio of PC to SAA, and $X_2$, which represents the type of SAA used. The dependent variables considered for this study were EE% ($Y_1$), PS ($Y_2$), PDI ($Y_3$), and ZP ($Y_4$). The design indicated a strong concurrence between the predicted and adjusted $R^2$ values, with the exception of the non-significant PDI. Furthermore, the predicted and adjusted $R^2$ values exhibited a minimal discrepancy of 0.2, indicating a strong alignment between the model's performance and the observed data [45]. The preference for a precision is for values larger than 4, as shown in table 3 [46].

**Table 3: Output data of the D-optimal analysis of Etho-LPs formulations and predicted and observed values for the selected Etho-LPs***

| Responses | EE% ($Y_1$) | PS (nm) ($Y_2$) | PDI ($Y_3$) | ZP (mV) ($Y_4$) |
|---|---|---|---|---|
| Adequate precision | 15.87 | 19.60 | 4.178 | 16.35 |
| Adjusted $R^2$ | 0.955 | 0.923 | 0.270 | 0.912 |
| Predicted $R^2$ | 0.846 | 0.902 | -0.710 | 0.869 |
| Significant factors | ($X_1$ and $X_2$) | ($X_1$ and $X_2$) | - | ($X_2$) |
| Predicted value of selected formulation | 92.17 | 99.59 | 0.363 | 36.09 |
| Observed value of selected formulation | 91.12±0.2 | 98.21±1.21 | 0.365±0.001 | 35.98 ±0.10 |
| Bias% | 1.15 | 1.40 | 0.54 | 0.30 |

*Composition of selected formulation (F14); PC: SAA molar ratio of 1:1.27 ($X_1$), 54.23: 40.02 mg/mg of CTAB and SA mixture as the SAA type ($X_2$). Abbreviations: EE%; Entrapment Efficiency Percentage, PS; Particle Size, PDI; Polydispersity Index, ZP; Zeta Potential, and Etho-Lps; Etho-leciplex. The data given in mean±SD.

### Effect of formulation variables on EE%

The significance of the independent variables X1 and X2 on the EE% of BRZ in the Etho-LP formulations shown in table 2 and fig. 1A.

For EE% values it ranged from 53.95±0.12 to 92.87±0.78 %, the high EE% of Etho-LPs was related to the hydrophobic nature of BRZ which leaded to successful incorporation within PC layers [27, 47]. ANOVA testing revealed that PC: SAA molar ratio ($X_1$) had significant effect ($p<0.0001$) on EE% of Etho-LPs. An observed fall in EE% values was observed with the increase in the proportion of cationic SAA suggesting a potential correlation between the solubilization of PC by SAA and the subsequent leakage of BRZ from Etho-LPs [26, 47]. Moreover, the increased viscosity imparted by increasing the proportion of PC might minimize the external diffusion and leakage of BRZ which in turn enhanced the %EE. The results were in agreement with Albash *et al.* who prepared moxifloxacin-loaded leciplex and found that the increase in (PC: CTAB) ratio from 1:1 to 5:1 led to an increase in EE% from 78.47 to 96.85%, respectively [26].

Regarding the SAA type ($X_2$), it was found that EE% values increased significantly ($p=0.049$) when utilizing CTAB compared to SA. The observed results can be attributed to the lipophilic nature of CTAB compared to SA, as indicated by their respective log P values. CTAB and SA have log P values of 8 and 7.7, respectively. This is in agreement with Carbone *et al.* [48].

### Effect of Formulation Variables on PS

The z-average diameter signifying the mean hydrodynamic diameter of the nanoparticles [49] is clarified in table 2 and graphically illustrated in fig. 1B. The PS of Etho-LPs ranged from 25.80±10.50 to 127.50±4.50 nm. The obtained PS values were suitable for ocular drug delivery as previously mentioned elsewhere [50].

ANOVA analysis of the results showed that both PC: SAA molar ratio ($X_1$) and SAA type ($X_2$) significantly affected the PS of Etho-LPs with p values of 0.0006, and 0.0003, respectively.

As illustrated in fig. 1B it was found that the PS decreased by increasing the SAA amount. This might be related to decreasing the interfacial tension by elevating SAA amount, resulting in the formation of smaller Etho-LPs. Comparable findings were observed in a previous study where stable oil-in-water nanoemulsions were prepared utilizing a non-ionic surfactant (Tween 40). It was discovered that the droplet size declined from 31.83 nm to 18.02 nm as the concentration of the surfactant was raised from 0.5 wt. % to 2.0 wt. % [51].

The use of SAA type ($X_2$) had a substantial impact on the PS of the Etho-LPs formed using CTAB, in comparison to those prepared using SA, where smaller PS values were obtained when using CTAB. The observed outcomes can be ascribed to the enhanced stabilizing effect of CTAB, as evidenced by the higher surface charge of CTAB Etho-LPs in comparison to SA Etho-LPs, which in turn reduced tendency of aggregation and fusion of particles. These findings align with the conclusions drawn by Varghese *et al.*, as they observed a correlation between the stabilizing properties of the cationic agent (Didodecyl Dimethyl Ammonium Bromide (DDAB)/1,2-Dioleoyl-3-trimethylammonium propane) and the PS of lecithin formulations. Where a rise in surface charge resulted in enhanced stabilizing capabilities, leading to a subsequent drop in PS [52].

### Effect of Formulation Variables on PDI

The PDI is a quantitative metric used to assess the width of unimodal size distributions. PDI values below 0.7 are considered acceptable; however, values beyond 0.7 have the potential to influence the stability of the formulation [47]. The PDI values are displayed in table 2 and depicted in fig. 2A.

The PDI values ranged from 0.318±0.11 to 0.523±0.10. The tested parameters, namely the PC: SAA molar ratio ($X_1$) and SAA type ($X_2$), exhibited a non-significant effect on the PDI, as evidenced by the p-values of 0.4152 and 0.4777, respectively. Based on the findings, it can be observed that the obtained PDI values were less than 0.7. These findings suggest that the Etho-LPs displayed a high level of homogeneity and narrow range of size distribution [47].

### Effect of formulation variables on ZP

ZP values were between 21.00±2.00 and 51.37±1.56 mV. Results are compiled in table 2 and plotted in fig. 2B. All Etho-LPs formulations had acceptable high positive ZP values indicating good stability, due to the presence of electrostatic repulsions between the dispersed particles [16]. The positive charge for Etho-LPs was due to the use of cationic SAA (CTAB and SA) [53, 54]. This positive charge serves to facilitate electrostatic interactions between the positively-charged Etho-LPs and negatively-charged sialic acid found in corneal mucins [19, 55].

ANOVA analysis of the obtained ZP values illustrated that the PC: SAA molar ratio ($X_1$) possessed a significant effect on ZP with p value of $<0.0001$ where increasing the proportion of cationic SAA resulted in an increase of ZP accordingly. The results obtained were consistent with the findings of Hassan *et al.*, who observed that all DDAB/CTAB leciplex formulations containing carvedilol exhibited a positive surface charge ranging from 31.6 to 53.9 mV, indicating excellent stability. For SAA type ($X_2$), the factor had no significant effect on ZP (p value = 0.065).
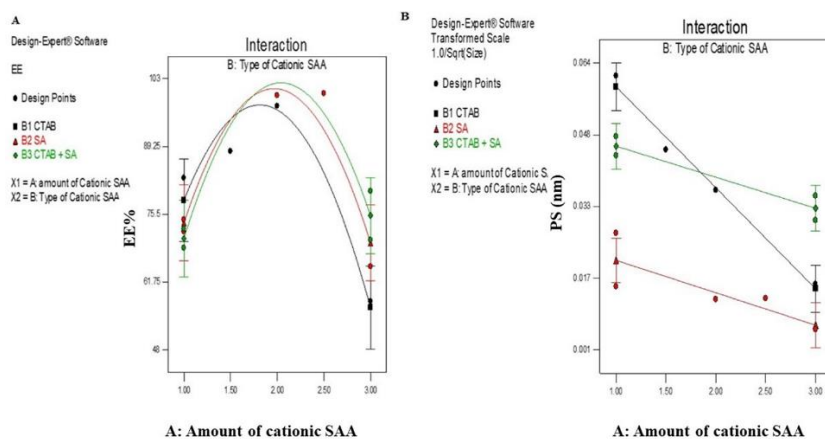
**Fig. 1: A) line plots for the effect of PC: SAA molar ratio and the type of SAA on EE%. B) Line plots for the effect of PC: SAA ratio and the type of SAA on PS, The data given in mean±SD**
**Abbreviations: PC: Phospholipid, SAA: Surface Active Agent, EE%: Entrapment Efficiency Percent, and PS: Particle Size**
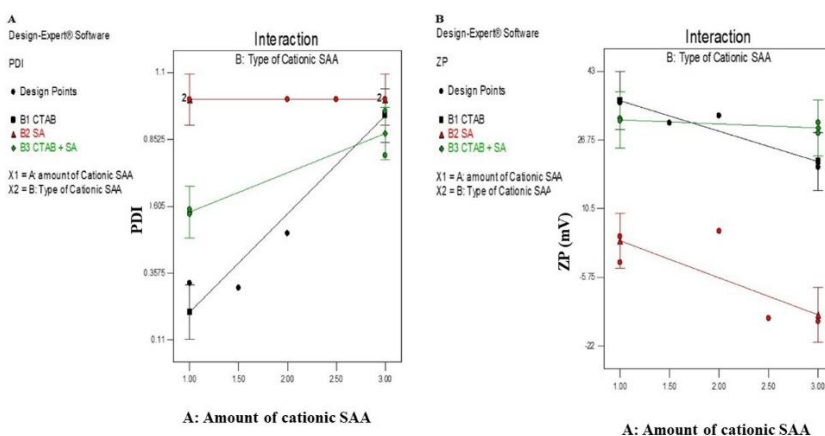


**Fig. 2: A) line plots for the effect of PC: SAA molar ratio and the type of SAA on PDI. B) line plots for the effect of PC: SAA ratio and the type of SAA on ZP, The data given in mean±SD**
**Abbreviations: PC: Phospholipid, SAA, Surface Active Agent, PDI: Polydispersity Index, and ZP; Zeta Potential**

**Selecting the optimum BRZ-Etho-LPs**

The different investigated factors were analyzed for the selection of optimum levels required for the preparation of a high-quality formulation. Etho-LPs were optimized through the desirability constraints in table 1. The optimum values of the variables were achieved through optimization based on a desirability function employing Design-Expert 7® software. The numerical analysis suggested an Etho-LPs formulation with an overall desirability value of 0.739. The suggested formulation (F14) was fabricated using PC: SAA molar ratio ($X_1$) of 1:1.27 molar ratio and CTAB and SA mixture as the SAA type ($X_2$;54.23: 40.02 w/w). The suggested formulation was prepared and evaluated as previously mentioned for its EE%, PS, PDI and ZP. The observed results for the aforementioned tests were 91.12±0.2 %, 76.21±1.21 nm, 0.421±0.001 and 35.88 ±0.10 mV, respectively. The predicted values for the previously mentioned tests were 92.08%, 75.03 nm, 0.422 and 35.98 mV, respectively. The high resemblance between the observed and predicted outcomes of the optimum Etho-LPs could presume the validity of the design to expect the responses (table 3). Furthermore, the average bias % values for all the obtained responses were less than 10% indicating the high model's predictability capacity [56].

***In vitro* release study**

The release of BRZ from the optimum Etho-LPs compared to BRZ suspension is shown in fig. 3. The results indicate a significant difference (p= 0.000) in the cumulative amount released of BRZ after 2 h (Q2) from the Etho-LPs (35.12±0.74%) compared to that of

released from BRZ suspension (7.08±0.05%). This initial flush from the Etho-LPs might be attributed to the dissolution of the surface drug in addition to the dissolution of PC in presence of SAA, which might lead to the formation of channels assisting the penetration of the release medium and hence drug dissolution [57, 58]. The initial flush was followed by a sustained release phase, representing the release of an entrapped drug inside the core of the nanoparticles [58], where the % BRZ released from the optimal Etho-LPs after 24 h (Q24) was significantly higher (72.05±0.73%) compared to the % drug released from the suspension (21.66±0.86%), with a p-value of 0.002. Higher Q24 values obtained from the optimized formulation might be endorsed to the enhanced solubility of the drug by the action of the used SAA [53].

This biphasic pattern is beneficial as the initial flush delivers an adequate amount of BRZ to the ocular tissues to exert its action, whereas the subsequent sustained phase preserves enough drug concentrations for extended periods of time. This sustained drug release decreases frequency of administration and hence enhance patients' compliance. The obtained results aligns with the findings stated by Abdellatif *et al.* [27].

**pH measurement**

Eye irritation and multiple daily administrations may hinder the clinical effectiveness of instilled eye drops; hence pH evaluation must be performed to ensure the feasibility of ocular application [59]. The acceptable pH values of eye drops can be between 3.5 and 8.5 [39, 60], with the typical value at 7.2±0. 2. The pH value of the

optimum Etho-LPs was 7.40±0.20, which is considered appropriate and suitable for ocular application. These findings are consistent with the research conducted by Abd-Elsalam *et al.*, during the development of mucoadhesive olaminosomes, where they observed that the pH values of the chosen formulations fell within the acceptable range of 3.7 to 5 [39].
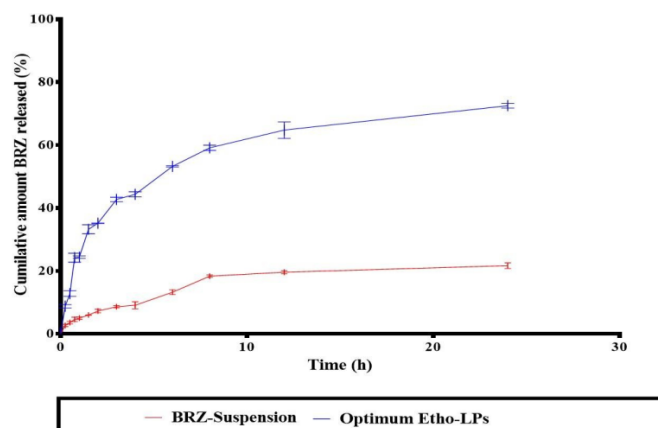


**Fig. 3:** *In vitro* release figure of BRZ suspension and the optimum Etho-LPs
**Abbreviations: BRZ; Brinzolamide, and Etho-LPs; Etho leciplex, the data given in mean±SD**

**Differential scanning calorimetry (DSC)**

The DSC thermograms are demonstrated in fig. 4. BRZ showed an endothermic peak equivalent to its melting point at 131 °C, which signifies the crystalline nature of the drug and is in line with the literature [61].The thermogram of the optimum Etho-LPs did not display the melting peak of BRZ. This might be due to that the effective entrapment of BRZ inside the Etho-LPs [62]. Additionally, the absence of BRZ characteristic peak in Etho-LPs could be attributed to the molecular dispersion of BRZ in Etho-LPs with the formation of solid solution, which resulted in the dilution of BRZ in a mixture and diminishing its characteristic peak [63].
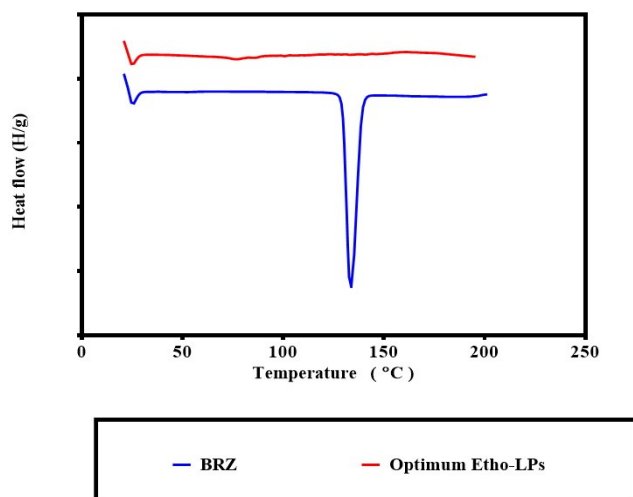


**Fig. 4: DSC thermograms of BRZ, and the optimum Etho-LPS**
**Abbreviations: DSC, Differential Scanning Calorimetry; BRZ, Brinzolamide, and Etho-LPs; Etho leciplex**
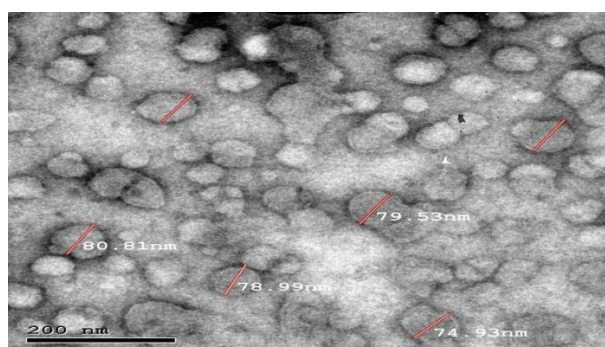


**Fig. 5: Transmission electron micrograph of the optimum Etho-LPs (scale bar: 200 nm)**
**Abbreviations: Etho-LPs; Etho leciplex**

**Transmission Electron Microscope (TEM)**

Morphological observations visualized that optimum Etho-LPs were spherical in shape (fig. 5). The PS values obtained from Zetasizer were in good harmony with TEM findings. In addition, no aggregations were observed, which might indicate the good dispersibility of the optimum Etho-LPs and this could be explained by the reasonable ZP on the Etho-LPs surfaces preventing the agglomeration of the prepared optimum Etho-LPs [16].

**Mucoadhesiontest**

The investigation of the interaction behavior between the optimum formulation and mucin is essential due to the significant role of mucin as a vital component of the eye. Conjunctival goblet cells are responsible for the production of mucin, which serves the purpose of moistening and safeguarding the ocular surface [63]. In order to assess the mucoadhesive characteristics of the optimized BRZ-loaded Etho-LPs under investigation, the formulation was combined with a solution of mucin. The findings of the study demonstrated a statistically significant alteration in ZP value of the optimized BRZ-loaded Etho-LPs formulation, which decreased from 35.98 ±0.10 to 27.60±0.40 mV. The observed decrease in ZP value can be ascribed to the ionic interaction between the amino groups, which carry a positive charge, of the used cationic surface-active agents (CTAB and SA), and the negatively charged sialic acid residues in mucin. This mucoadhesion can prolong the residence of the applied drug, hence enhancing its bioavailability by enhancing the availability of the drug at the specific site of application [39].

**Effect of short-term storage**

At the end of the storage period of 3 mo at 4±2 °C, the stored optimum Etho-LPs didn't display any aggregates in comparison to fresh ones. The values of EE%, PS, PDI, and ZP for stored optimum Etho-LPs were 91.99±0.1%, 78.00±5.00 nm, 0.423±0.001, and 35.77±1.33 mV, respectively. No statistical differences were detected between the fresh and stored samples ($p>0.05$). These results were in agreement with Date A *et al.*, who observed that the quercetin-recipes did not show any significant change in the PS and PDI when stored at refrigerated conditions [31].

***In vivo* studies**

The efficacy of the optimum BRZ-loaded Etho-LPs was tested in comparison to BRZ suspension both administered at one single dose of 10 mg/ml by calculating the pharmacokinetic parameters of the drug in the tear film. Table 4 and fig. 6 illustrate the tear film concentration-time curve besides the pharmacokinetic parameters for both samples. Both the table and fig. present the superiority of the optimum BRZ-loaded Etho-LPs over drug suspension. The $C_{max}$ values for the investigated formulation and drug suspension were 6755.00±2322.43 and 1937.50±78.04 ng/ml (p value<0.05), respectively, reached after 1 and 0.75 h, in that order. Regarding the $AUC_{0-24}$ values, it was manifested that the optimum Etho-LPs possessed significantly higher values compared to drug suspension (p-value = 0.029). The obtained values for the aforementioned formulations were 40130.00±13689.50 versus 12940.43±8506.44 ng. h/ml, respectively. From the aforementioned findings, it can be determined that the optimum Etho-LPs enhanced the drug bioavailability in ocular tissues. This might be attributed to the small nano size of the prepared Etho-LPs, which in turn enhanced the penetration via ocular tissues [64, 65]. Moreover, this improvement can be ascribed to the utilization of cationic surfactants that promote the attachment of Etho-LPs to the negatively charged sialic acid groups present in the mucus membrane of the corneal surface. As a consequence, there was an increase in corneal retention, leading to a reduction in drug elimination through tear flow and an enhancement in transcorneal flux [27]. On the other hand, a previous study illustrated that the presence of PC in the composition of nanocarriers might forma drug reservoir for consequent ocular penetration due to its possible capability of protecting the drug-loaded nanocarriers from tear lysozyme and esterase action and, hence better drug bioavailability [66].

**Table 4: The pharmacokinetic parameters of BRZ after the administration of optimum Etho-LPs\* and drug suspension into rabbits' eyes**

| Pharmacokinetic parameter | Optimum Etho-LPs | Drug suspension |
|---|---|---|
| $C_{max}$ (ng/ml) | 6755.00±2322.43 | 1937.50±78.04 |
| $T_{max}$** (h) | 1 | 0.75 |
| $AUC_{0-24}$(ng. h/ml) | 40130.00±13689.50 | 12940.43±8506.44 |

*Composition of optimum Etho-LPs; PC: SAA molar ratio of 1:1.27 ($X_1$), 54.23: 40.02 mg/mg of CTABand SA mixture as the SAA type ($X_2$). **$T_{max}$ values calculated as median. Abbreviations: BRZ; Brinzolamide, and Etho-Lps; Etho-Leciplex. The data given in mean±SD.
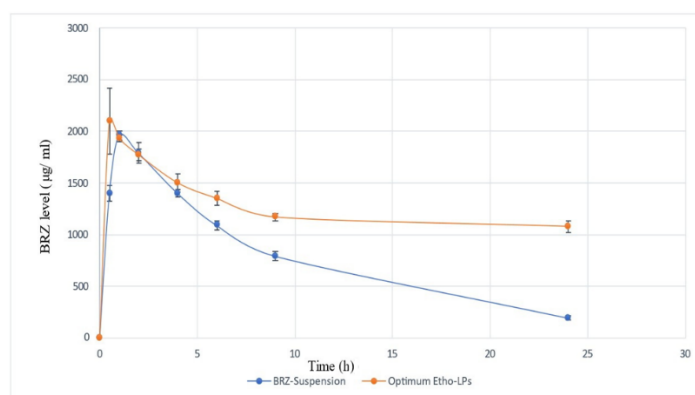


**Fig. 6: Mean BRZ tear concentration-time curve for BRZ suspension and the optimum Etho-LPs in rabbits' eyes, the data given in mean±SD Abbreviations: BRZ; Brinzolamide, and Etho-LPs; Etho leciplex**

**Histopathological study**

Microscopic examination of the treated eyes of male Albino rabbits showed no histopathological changes in the inspected sections of the cornea, iris, retina or sclera compared to the control (fig. 7). The results demonstrated the safety of the optimum Etho-LPs even after intensive use. Moreover, the obtained results indicated the safety and biocompatibility of the used components on the ocular tissues. Similar studies in literature stated the safety of PC [67], CTAB [68] and SA [69] when applied on ocular tissues.
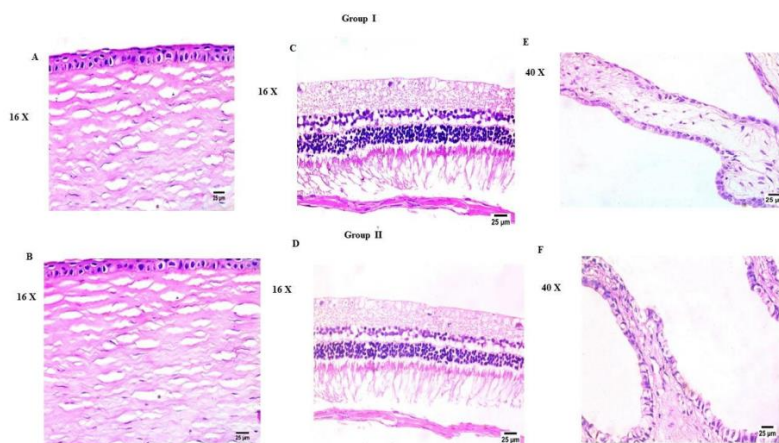
Fig. 7: Photomicrographs showing histopathological sections (hematoxylin and eosin stained) of untreated group I and treated optimum Etho-LPs group II rabbits' eyes. A and B illustrate the histological structure of the cornea (16X), (C, D) illustrates the histological structure of the retina, choroid, and sclera (16X), and (E-F) illustrates histological structure of the retina, choroid, and sclera (40X)
Abbreviations: BRZ; Brinzolamide, and Etho-LPs; Etho leciplex

## CONCLUSION

Brinzolamide (BRZ) loaded Etho-Leciplex (Etho-LPs) were fabricated by a simple one-step technique using different molar ratios of phospholipid (PC) and cationic surfactants mixture of cetyltrimethylammonium bromide (CTAB), and stearyl amine (SA) applying D-optimal design. The suggested optimum Etho-LPs, after statistical analysis, consisted of 1:1.27 as PC: SAA molar ratio ($X_1$) and both CTAB combined with SA as the SAA type ($X_2$). The optimum Etho-LPs were spherical-shaped with excellent entrapment efficiency of 91.12±0.2 %, particle size value of 76.21±1.21 nm, besides the particles possessed narrow particle size distribution with polydispersity index value of 0.421±0.001, and zeta potential of 35.88 ±0.10 mV. Moreover, the *in vitro* release studies showed the enhancement of drug release after 24 h compared to BRZ suspension. The use of the cationic surfactants imparted positive charges on the formulated Etho-LPs which in turn enhanced their mucoadhesive properties required for extending the contact time on the ocular tissues. Based on the outcomes of *in vivo* pharmacokinetic study, the optimum Etho-LPs formulation presented a significant enhancement in bioavailability of BRZ compared to the BRZ suspension. Furthermore, histopathological assessment of Etho-LPs treated group showed no histopathological abnormalities in the examined sections of the cornea, iris, retina or sclera compared to the untreated group. These outcomes indicated that Etho-LPs are promising ocular nanocarriers for hydrophobic drugs.

## FUNDING

## AUTHORS CONTRIBUTIONS

Conceptualization, Sara Nageeb El-Helaly, Mina I. Tadros, and Nermeen A. Elkasabgy. Formal analysis, Sara Nageeb El-Helaly, Hayder A. Hammoodi, Mina I. Tadros, and Nermeen A. Elkasabgy. Investigation, Sara Nageeb El-Helaly, Hayder A. Hammoodi, Mina I. Tadros, Nermeen A. Elkasabgy. Resources, Sara Nageeb El-Helaly, Mina I. Tadros, Nermeen A. Elkasabgy Writing—original draft preparation, Sara Nageeb El-Helaly, Hayder A. Hammoodi, Nermeen A. Elkasabgy. Writing—review and editing, Sara Nageeb El-Helaly, Mina I. Tadros, and Nermeen A. Elkasabgy. Supervision, Sara Nageeb El-Helaly, Mina I. Tadros, Nermeen A. Elkasabgy. All authors have read and agreed to the published version of the manuscript.

## CONFLICTS OF INTERESTS

The authors declare no conflict of interest.

## REFERENCES

1. Shukr MH, Ismail S, El-hossary GG, El-shazly AH. Design and evaluation of mucoadhesive in situ liposomal gel for sustained ocular delivery of travoprost using two steps factorial design. J Drug Deliv Sci Technol. 2021;1(61):102333. doi: 10.1016/j.jddst.2021.102333.

2. Maier PC, Funk J, Schwarzer G, Antes G, Falck Ytter YT. Treatment of ocular hypertension and open-angle glaucoma: a meta-analysis of randomised controlled trials. BMJ. 2005;331(7509):134. doi: 10.1136/bmj.38506.594977.E0, PMID 15994659.

3. Bengtsson B, Leske MC, Hyman L, Heijl A, Early Manifest Glaucoma Trial Group. Fluctuation of intraocular pressure and glaucoma progression in the early manifest glaucoma trial. Ophthalmology. 2007;114(2):205-9. doi: 10.1016/j.ophtha.2006.07.060, PMID 17097736.

4. Conlon R, Saheb H, Ahmed II. Glaucoma treatment trends: a review. Can J Ophthalmol. 2017;52(1):114-24. doi: 10.1016/j.jcjo.2016.07.013, PMID 28237137.

5. Linden C, Alm A. Prostaglandin analogues in the treatment of glaucoma. Drugs Aging. 1999;14(5):387-98. doi: 10.2165/00002512-199914050-00006, PMID 10408738.

6. Tejwani S, Machiraju P, Nair AP, Ghosh A, Das RK, Ghosh A. Treatment of glaucoma by prostaglandin agonists and beta-blockers in combination directly reduces pro-fibrotic gene expression in trabecular meshwork. J Cell Mol Med. 2020;24(9):5195-204. doi: 10.1111/jcmm.15172, PMID 32267082.

7. Supuran CT, Altamimi AS, Carta F. Carbonic anhydrase inhibition and the management of glaucoma: a literature and patent review 2013-2019. Expert Opin Ther Pat. 2019;29(10):781-92. doi: 10.1080/13543776.2019.1679117, PMID 31596641.

8. Nocentini A, Supuran CT. Adrenergic agonists and antagonists as antiglaucoma agents: a literature and patent review (2013-2019). Expert Opin Ther Pat. 2019;29(10):805-15. doi: 10.1080/13543776.2019.1665023, PMID 31486689.

9. Jain N, Verma A, Jain N. Formulation and investigation of pilocarpine hydrochloride niosomal gels for the treatment of glaucoma: intraocular pressure measurement in white albino rabbits. Drug Deliv. 2020;27(1):888-99. doi: 10.1080/10717544.2020.1775726, PMID 32551978.

10. Yadav KS, Rajpurohit R, Sharma S. Glaucoma: current treatment and impact of advanced drug delivery systems. Life Sci. 2019;221:362-76. doi: 10.1016/j.lfs.2019.02.029, PMID 30797820.

11. Winum JY, Casini A, Mincione F, Starnotti M, Montero JL, Scozzafava A. Carbonic anhydrase inhibitors: N-(p-sulfamoylphenyl)-alpha-D-glycopyranosylamines as topically acting antiglaucoma agents in hypertensive rabbits. Bioorg Med Chem Lett. 2004;14(1):225-9. doi: 10.1016/j.bmcl.2003.09.063, PMID 14684332.

12. Sulatha VB, Krishna R, Akshay HT. Brinzolamide-induced eye discharge: a rare entity. Asian J Pharm Clin Res. 2016;9(2):1-2.

13. Gohil R. Optimization of brinzolamide loaded microemulsion using formulation by design approach: characterization and *in vitro* evaluation. Curr Drug Ther. 2020;15(1):37-52. doi: 10.2174/22123903OTU1zOTc6TcVY.

14. Zhou Y, Fang A, Wang F, Li H, Jin Q, Huang L. Core-shell lipid-polymer nanoparticles as a promising ocular drug delivery system to treat glaucoma. Chinese Chemical Letters. 2020;31(2):494-500. doi: 10.1016/j.cclet.2019.04.048.

15. Younes NF, Abdel-halim SA, Elassasy AI. Solutol HS15 based binary mixed micelles with penetration enhancers for augmented corneal delivery of sertaconazole nitrate: optimization, *in vitro*, ex vivo and *in vivo* characterization. Drug Deliv. 2018;25(1):1706-17. doi: 10.1080/10717544.2018.1497107, PMID 30442039.

16. Raj VK, Mazumder RU, Madhra MO. Ocular drug delivery system: challenges and approaches. Int J App Pharm. 2020;12:49-57. doi: 10.22159/ijap.2020v12i5.38762.

17. Younes NF, Abdel Halim SA, Elassasy AI. Corneal targeted sertaconazole nitrate loaded cubosomes: preparation, statistical optimization, *in vitro* characterization, ex vivo permeation and *in vivo* studies. Int J Pharm. 2018;553(1-2):386-97. doi: 10.1016/j.ijpharm.2018.10.057, PMID 30393167.

18. Abdelbary GA, Amin MM, Zakaria MY. Ocular ketoconazole-loaded proniosomal gels: formulation, ex vivo corneal permeation and *in vivo* evaluation. Drug Deliv. 2017;24(1):309-19. doi: 10.1080/10717544.2016.1247928, PMID 28165809.

19. Hassan DH, Abdelmonem R, Abdellatif MM. Formulation and characterization of carvedilol leciplex for glaucoma treatment: *in vitro*, ex-vivo and *in vivo* study. Pharmaceutics. 2018;10(4):197. doi: 10.3390/pharmaceutics10040197, PMID 30347876.

20. Ustundag Okur N, Homan Gokce E. Lipid nanoparticles for ocular drug delivery. Int J Ophthal Res. 2015;1(3):77-82. doi: 10.17554/j.issn.2409-5680.2015.01.29.

21. Suri R, Beg S, Kohli K. Target strategies for drug delivery bypassing ocular barriers. J Drug Deliv Sci Technol. 2020;55. doi: 10.1016/j.jddst.2019.101389.

22. Das B, Nayak AK, Mallick S. Lipid-based nanocarriers for ocular drug delivery: an updated review. J Drug Deliv Sci Technol. 2022;76. doi: 10.1016/j.jddst.2022.103780.

23. Sanchez Lopez E, Espina M, Doktorovova S, Souto EB, Garcia ML. Lipid nanoparticles (SLN, NLC): overcoming the anatomical and physiological barriers of the eye-Part II-ocular drug-loaded lipid nanoparticles. Eur J Pharm Biopharm. 2017;110:58-69. doi: 10.1016/j.ejpb.2016.10.013, PMID 27789359.

24. Albash R, M Abdellatif M, Hassan M, M Badawi N. Tailoring terpesomes and leciplex for the effective ocular conveyance of moxifloxacin hydrochloride (comparative assessment): *in vitro*, ex-vivo, and *in vivo* evaluation. Int J Nanomedicine. 2021;16:5247-63. doi: 10.2147/IJN.S316326, PMID 34376978.

25. Yuan H, Ma Q, Ye l, Piao G. The traditional medicine and modern medicine from natural products. Molecules. 2016;21(5):559. doi: 10.3390/molecules21050559, PMID 27136524

26. Neeraj J, V Anurag NJ. Preformulation studies of niosomal gel containing dipivefrin hydrochloride for antiglaucomatic activity. Int J Pharm Pharm Sci. 2024;16(2):1-7.

27. Pankaj KJ, Shikha K, Tapash C. Lipid-polymer hybrid nanocarriers as a novel drug delivery platform. Int J Pharm Pharm Sci. 2022;12(4):1-12.

28. Abdellatif MM, Josef M, El-Nabarawi MA, Teaima M. Sertaconazole-nitrate-loaded leciplex for treating keratomycosis: optimization using d-optimal design and *in vitro*, ex vivo, and *in vivo* studies. Pharmaceutics. 2022;14(10). doi: 10.3390/pharmaceutics14102215, PMID 36297650.

29. Date AA, Srivastava D, Nagarsenker MS, Mulherkar R, Panicker L, Aswal V. Lecithin-based novel cationic nanocarriers (LeciPlex) I: fabrication, characterization and evaluation. Nanomedicine. 2011;6(8):1309-25. doi: 10.2217/nnm.11.38, PMID 22026377.

30. Dhawan VV, Joshi GV, Jain AS, Nikam YP, Gude RP, Mulherkar R. Apoptosis induction and anti-cancer activity of leciplex formulations. Cell Oncol (Dordr). 2014;37(5):339-51. doi: 10.1007/s13402-014-0183-7, PMID 25204961.

31. Shah SM, Ashtikar M, Jain AS, Makhija DT, Nikam Y, Gude RP. LeciPlex, invasomes, and liposomes: a skin penetration study. Int J Pharm. 2015;490(1-2):391-403. doi: 10.1016/j.ijpharm.2015.05.042, PMID 26002568.

32. Date AA, Nagarsenker MS, Patere S, Dhawan V, Gude RP, Hassan PA. Lecithin-based novel cationic nanocarriers (leciplex) ii: Improving therapeutic efficacy of quercetin on oral administration. Mol Pharm. 2011;8(3):716-26. doi: 10.1021/mp100305h, PMID 21480639.

33. Elmowafy M, Shalaby K, Alruwaili NK, Elkomy MH, Zafar A, Soliman GM. EthoLeciplex: a new tool for effective cutaneous delivery of minoxidil. Drug Dev Ind Pharm. 2022;48(9):457-69. doi: 10.1080/03639045.2022.2124261, PMID 36093810.

34. Abo Elela MM, Elkasabgy NA, Basalious EB. Bio-shielding in situ forming gels (BSIFG) loaded with liposheres for depot injection of quetiapine fumarate: *in vitro* and *in vivo* evaluation. AAPS PharmSciTech. 2017;18(8):2999-3010. doi: 10.1208/s12249-017-0789-y, PMID 28493003.

35. El Taweel MM, Aboul-Einien MH, Kassem MA, Elkasabgy NA. Intranasal zolmitriptan-loaded bilosomes with extended nasal mucociliary transit time for direct nose to brain delivery. Pharmaceutics. 2021;13(11):1828. doi: 10.3390/pharmaceutics13111828, PMID 34834242.

36. Albash R, Badawi NM, Hamed MI, Ragaie MH, Mohammed SS, Elbesh RM. Exploring the synergistic effect of bergamot essential oil with spironolactone loaded nano-phytosomes for treatment of acne vulgaris: *in vitro* optimization, in silico studies, and clinical evaluation. Pharmaceuticals (Basel). 2023;16(1):128. doi: 10.3390/ph16010128, PMID 36678625.

37. Albash R, Ragaie MH, Hassab MA, El-Haggar R, Eldehna WM, Al-Rashood ST. Fenticonazole nitrate loaded trans-novasomes for effective management of tinea corporis: design characterization, in silico study, and exploratory clinical appraisal. Drug Deliv. 2022;29(1):1100-11. doi: 10.1080/10717544.2022.2057619, PMID 35373684.

38. Zeb A, Ullah K. Development *in vitro* and *in vivo* evaluation of ezetimibe-loaded solid lipid nanoparticles and their comparison with marketed product. J Drug Deliv Sci Technol. 2019;1(51):583-90. doi: 10.1016/j.jddst.2019.02.026.

39. Zaghloul N, El Hoffy NM, Mahmoud AA, Elkasabgy NA. Cyclodextrin stabilized freeze-dried silica/chitosan nanoparticles for improved terconazole ocular bioavailability. Pharmaceutics. 2022;14(3):470. doi: 10.3390/pharmaceutics14030470, PMID 35335847.

40. Abd-elsalam WH, Elkasabgy NA. Mucoadhesive olaminosomes: a novel prolonged release nanocarrier of agomelatine for the treatment of ocular hypertension. Int J Pharm. 2019;560:235-45. doi: 10.1016/j.ijpharm.2019.01.070, PMID 30763680.

41. El-Naggar MM, El-Nabarawi MA, Teaima MH, Hassan M, Hamed MI, Elrashedy AA. Integration of terpesomes loaded levocetrizine dihydrochloride gel as a repurposed cure for methicillin-resistant staphylococcus aureus (MRSA)-induced skin infection; d-optimal optimization, ex-vivo, in-silico, and *in vivo* studies. Int J Pharm. 2023;633:122621. doi: 10.1016/j.ijpharm.2023.122621, PMID 36693486.

42. Roggeband R, York M, Pericoi M, Braun W. Eye irritation responses in rabbit and man after single applications of equal volumes of undiluted model liquid detergent products. Food Chem Toxicol. 2000;38(8):727-34. doi: 10.1016/s0278-6915(00)00057-0, PMID 10908820.

43. Jiang S, Chappa AK, Proksch JW. A rapid and sensitive LC/MS/MS assay for the quantitation of brimonidine in ocular fluids and tissues. J Chromatogr B Analyt Technol Biomed Life Sci. 2009;877(3):107-14. doi: 10.1016/j.jchromb.2008.11.009, PMID 19109079.

44. Baneux PJ, Garner D, McIntyre HB, Holshuh HJ. Euthanasia of rabbits by intravenous administration of ketamine. J Am Vet Med Assoc. 1986;189(9):1038-9, PMID 3505922.

45. Fang G, Wang Q, Yang X. Physicochemical and engineering aspects vesicular phospholipid gels as topical ocular delivery system for treatment of anterior uveitis. Colloids Surf a Physicochem. 2021;20:627, 127187. doi: 10.1016/j.colsurfa.2021.127187.

46. Baig MS, Owida H, Njoroge W, Siddiqui AR, Yang Y. Development and evaluation of cationic nanostructured lipid carriers for ophthalmic drug delivery of besifloxacin. J Drug Deliv Sci Technol. 2020;55. doi: 10.1016/j.jddst.2019.101496.

47. Joseph J, BN VH, D RD. Experimental optimization of lornoxicam liposomes for sustained topical delivery. Eur J Pharm Sci. 2018;112:38-51. doi: 10.1016/j.ejps.2017.10.032, PMID 29111151.

48. Emad A, Salah S, Amer MS, Elkasabgy NA. 3D nanocomposite alginate hydrogel loaded with pitavastatin nanovesicles as a functional wound dressing with controlled drug release; preparation, *in vitro* and *in vivo* evaluation. J Drug Deliv Sci Technol. 2022;1(71):103292. doi: 10.1016/j.jddst.2022.103292.

49. Salama A, Badran M, Elmowafy M, Soliman GM. Spironolactone-loaded leciplexes as potential topical delivery systems for female acne: *in vitro* appraisal and ex vivo skin permeability studies. Pharmaceutics. 2019;12(1):25. doi: 10.3390/pharmaceutics12010025, PMID 31881783.

50. Carbone C, Tomasello B, Ruozi B, Renis M, Puglisi G. Preparation and optimization of PIT solid lipid nanoparticles via statistical factorial design. Eur J Med Chem. 2012;49:110-7. doi: 10.1016/j.ejmech.2012.01.001, PMID 22244589.

51. Das S, Ng WK, Tan RB. Are nanostructured lipid carriers (NLCs) better than solid lipid nanoparticles (SLNs): development, characterizations and comparative evaluations of clotrimazole-loaded SLNs and NLCs? Eur J Pharm Sci. 2012;47(1):139-51. doi: 10.1016/j.ejps.2012.05.010, PMID 22664358. ejps.2012.05.010.

52. Bachu RD, Chowdhury P, Al-saedi ZH, Karla PK, Boddu SH. Ocular drug delivery barriers-role of nanocarriers in the treatment of anterior segment ocular diseases. Pharmaceutics. 2018;10(1):1-31. doi: 10.3390/pharmaceutics10010028, PMID 29495528.

53. Onaizi SA. Characteristics and pH-responsiveness of SDBS-stabilized crude oil/water nanoemulsions. Nanomaterials (Basel). 2022;12(10). doi: 10.3390/nano12101673, PMID 35630894.

54. Varghese SE, Fariya MK, Rajawat GS, Steiniger F, Fahr A, Nagarsenker MS. LecithinLecithin and PLGA-based self-assembled nanocomposite, Lecithmer: preparation, characterization, and pharmacokinetic/pharmacodynamic evaluation. Drug Deliv Transl Res. 2016;6(4):342-53. doi: 10.1007/s13346-016-0314-y, PMID 27371394.

55. Mei Z, Liu S, Wang L, Jiang J, Xu J, Sun D. Preparation of positively charged oil/water nano-emulsions with a sub-PIT method. J Colloid Interface Sci. 2011;361(2):565-72. doi: 10.1016/j.jcis.2011.05.011.

56. Adel IM, Elmeligy MF, Abdelrahim ME, Maged A, Abdelkhalek AA, Abdelmoteleb AM. Design and characterization of spray-dried proliposomes for the pulmonary delivery of curcumin. Int J Nanomedicine. 2021;16:2667-87. doi: 10.2147/IJN.S306831, PMID 33854314.

57. Apaolaza PS, Delgado D, del Pozo-Rodriguez A, Gascon AR, Solinis MA. A novel gene therapy vector based on hyaluronic acid and solid lipid nanoparticles for ocular diseases. Int J Pharm. 2014;465(1-2):413-26. doi: 10.1016/j.ijpharm.2014.02.038, PMID 24576595.

58. Abdel Hafez SM, Hathout RM, Sammour OA. Tracking the transdermal penetration pathways of optimized curcumin-loaded chitosan nanoparticles via confocal laser scanning microscopy. Int J Biol Macromol. 2018;108:753-64. doi: 10.1016/j.ijbiomac.2017.10.170, PMID 29104049.

59. Kamel R, El-Wakil NA, Abdelkhalek AA, Elkasabgy NA. Topical cellulose nanocrystals-stabilized nanoemulgel loaded with ciprofloxacin HCl with enhanced antibacterial activity and tissue regenerative properties. J Drug Deliv Sci Technol. 2021;64:102553. doi: 10.1016/j.jddst.2021.102553.

60. Loftsson T, Jansook P, Stefansson E. Topical drug delivery to the eye: dorzolamide. Acta Ophthalmol. 2012;90(7):603-8. doi: 10.1111/j.1755-3768.2011.02299.x, PMID 22269010.

61. Mathis G. Clinical ophthalmic pharmacology and therapeutics: ocular drug delivery. Vet Ophthalmol. 1999:291-7.

62. Vo A, Feng X, Patel D, Mohammad A, Patel M, Zheng J. *In vitro* physicochemical characterization and dissolution of brinzolamide ophthalmic suspensions with similar composition. Int J Pharm. 2020;588:119761. doi: 10.1016/j.ijpharm.2020.119761, PMID 32795488.

63. Adel IM, Elmeligy MF, Amer MS, Elkasabgy NA. Polymeric nanocomposite hydrogel scaffold for jawbone regeneration: the role of rosuvastatin calcium-loaded silica nanoparticles. Int J Pharm X. 2023;6:100213. doi: 10.1016/j.ijpx.2023.100213, PMID 37927584.

64. Gipson IK. Goblet cells of the conjunctiva: a review of recent findings. Prog Retin Eye Res. 2016;54:49-63. doi: 10.1016/j.preteyeres.2016.04.005, PMID 27091323.

65. Weng Y, Liu J, Jin S, Guo W, Liang X, Hu Z. Nanotechnology-based strategies for treatment of ocular disease. Acta Pharm Sin B. 2017;7(3):281-91. doi: 10.1016/j.apsb.2016.09.001, PMID 28540165.

66. Hospital CU, Province J, Province J, Efficient D. Nanoparticles in the ocular drug delivery. Int J Ophthalmol. 2013;6(3):390-6. doi: 10.3980/j.issn.2222-3959.2013.03.25.

67. Araujo J, Gonzalez E, Egea MA, Garcia ML, Souto EB. Nanomedicines for ocular NSAIDs: safety on drug delivery. Nanomedicine. 2009;5(4):394-401. doi: 10.1016/j.nano.2009.02.003, PMID 19341814.

68. Fang G, Wang Q, Yang X, Qian Y, Zhang G, Zhu Q. Vesicular phospholipid gels as topical ocular delivery system for treatment of anterior uveitis. Colloids and Surfaces A: Physicochemical and Engineering Aspects. 2021;627. doi: 10.1016/j.colsurfa.2021.127187.

69. Fangueiro JF, Andreani T, Egea MA, Garcia ML, Souto SB, Silva AM. Design of cationic lipid nanoparticles for ocular delivery: development, characterization and cytotoxicity. Int J Pharm. 2014;461(1-2):64-73. doi: 10.1016/j.ijpharm.2013.11.025, PMID 24275449.

70. Alhakamy NA, Hosny KM, Aldryhim AY, Rizg WY, Eshmawi BA, Bukhary HA. Development and optimization of ofloxacin as solid lipid nanoparticles for enhancement of its ocular activity. J Drug Deliv Sci Technol. 2022;72:103373. doi: 10.1016/j.jddst.2022.103373.